

The Baryon Anomaly and Strong Color Fields at LHC in Pb+Pb at 2.76A TeV.

V. Topor Pop,¹ M. Gyulassy,² J. Barrette,¹ and C. Gale¹

¹*McGill University, Montreal, H3A 2T8, Canada*

²*Columbia University, New York, N.Y. 10027, USA*

(Dated: June 29, 2011)

Abstract

With the HIJING/B \bar{B} v2.0 heavy ion event generator, we explore the phenomenological consequences of several high parton density dynamical effects predicted in central Pb+Pb collisions at the Large Hadron Collider (LHC) energies. These include (1) jet quenching due to parton energy loss (dE/dx), (2) strangeness and hyperon enhancement due to strong *longitudinal* color field (SCF), and (3) enhancement of baryon-to-meson ratios due to baryon-anti-baryon junctions (J \bar{J}) loops and SCF effects. The saturation/minijet cutoff scale $p_0(s)$ and effective string tension $\kappa(s, A)$ are constrained by our previous analysis of LHC p+p data and recent data on the charged multiplicity for Pb+Pb collisions reported by the ALICE collaboration. We predict the hadron flavor dependence (mesons and baryons) of the nuclear modification factor $R_{AA}(p_T)$ and emphasize the possibility that the baryon anomaly could persist at the LHC up to $p_T \sim 10$ GeV, well beyond the range observed in central Au+Au collisions at RHIC energies.

PACS numbers: 12.38.Mh, 24.85.+p, 25.75.-q

I. INTRODUCTION

With the commissioning of the Large Hadron Collider (LHC), it is now possible to test dynamical models of multiparticle production in nuclear collisions up to a center-of-mass energy (c.m.) per nucleon $\sqrt{s_{\text{NN}}} = 5.5$ TeV. Charged particle densities at mid-pseudorapidity, $(2dN_{\text{ch}}/d\eta)/N_{\text{part}}$, and their dependence on energy and centrality are important for understanding the mechanism of hadron production and especially the interplay of soft (string fragmentation) and hard (perturbative QCD) scattering contributions at an order of magnitude higher energies than were extensively studied up to now at the Relativistic Heavy Ion Collider (RHIC/BNL). The rate of parton-parton and multi parton-parton scattering and soft processes are strongly correlated with the observed particle multiplicity (related to the *initial entropy* and the *initial energy density* generated in nuclear collisions over spacetime volumes up to 10^4 greater than in elementary p+p collisions).

Using the constraints on dynamical parameters from data at RHIC energies, there remain relatively large uncertainties (\sim a factor of two) on predictions for charged hadron multiplicities at the LHC energies: see Refs. [1–16]. The first data on inclusive charged particle distributions from the LHC in Pb+Pb collisions are now available [17–22]. Recently, ATLAS analyzed event samples from central (0-10%) Pb+Pb collisions at $\sqrt{s_{\text{NN}}} = 2.76$ TeV in which the transverse energy of the most energetic jet (leading jet) $E_{T_1} > 100$ GeV and where a recoiling jet with transverse energy $E_{T_2} > 25$ GeV could be found at azimuthal separation $\Delta\Phi > \pi/2$. In comparison with pp collisions, ATLAS observed (within a narrow cone) in Pb+Pb collisions a strong reduction of the number of recoiling jets carrying a large fraction of the maximum available jet energy $x = E_{T_2}/E_{T_1} > 0.6$ [21]. This, is consistent with the expected strong quenching of jets due to partonic energy loss in ultra-dense quark gluon plasma (QGP). In addition to the tomographic interest in jet quenching high p_T observables, there is considerable interest on the impact of mini-jet quenching as an additional final state interaction source of the observed bulk multiplicity/entropy production. The LHC data on nucleus-nucleus ($A + A$) collisions may lead to an improved theoretical understanding of ultra-dense multiparton plasma based on a Quantum Chromodynamics (QCD) approach [9, 10, 23–25].

To isolate quark-gluon plasma signatures in heavy-ion collision data, it is imperative to work in a framework that can simultaneously account for nucleon-nucleon collisions ($p + p$)

in the same energy range. In fact $p + p$ reactions can not be considered as elementary at the LHC and their study have already revealed possible interesting new physics [26]. We utilize the HIJING/B \bar{B} 2.0 heavy ion generator as a phenomenological tool that can systematically relate observables in $p+p$, $p+A$, and $A+A$ collisions in terms of a common framework based on a two component picture of the dynamics involving soft longitudinal beam jets, multiple mini jets, and rare hard pQCD processes. The Monte Carlo code inherits the phenomenological successes of the LUND [27] and Dual Parton Model (DPM) [28] string excitation and hadronization mechanisms as well as the hard processes encoded in the PYTHIA [29] event generator. Multiple low $p_T < Q_s(x, A)$ transverse momentum color exchanges excite the incident baryons into longitudinal strings that fragment due to color neutralization into an array of physical hadron resonance states. Hard processes are modelled as high p_T kinks in the strings and hadronize via the well tested LUND scheme in e^+e^- and ep processes. HIJING model [30] uses a variant of the string excitation LUND and DPM models constrained to lower energy pp data.

In heavy ion collisions, the novel “nuclear physics” is due to the nuclear modification of the parton distribution functions, the possibility of multiple longitudinal flux tube overlapping leading to strong longitudinal color field (SCF) effects referred to as color ropes or glasma. Strong fields also lead to enhanced strangeness production [31]. The effect is especially enhanced for production of baryons with multiple strange quarks as discovered first at the SPS/CERN [32]. Recently, the data on the production of strange particles with one, two or more strange quarks for $p + \bar{p}$ collisions at the Tevatron [33] and for $p + p$ collisions at the LHC [34, 35] have been reported. In reference [33] it was shown that the ratio Ξ^-/Λ and Ω^-/Λ rise at low p_T and the ratio reaches an unexpected plateau at $p_T > 4$ GeV/ c , which persist up to rather large 10 GeV/ c . This result is a major motivation for the present work.

We address these and other issues within the framework of the HIJING/B \bar{B} v2.0 model [36–38]. A systematic comparison with data on $p+p$ and $p+\bar{p}$ collisions in a wide energy range [36] revealed that minijet production and fragmentation as implemented in the HIJING/B \bar{B} v2.0 model provide a simultaneous and consistent explanation of several effects: the inclusive spectra at moderate transverse momentum ($p_T < 5$ GeV/ c), the energy dependence of the central rapidity density, the (strange)baryon-mesons ratios and the baryon-anti-baryon asymmetry. Specifically, in this paper we extend our studies to the dynamic consequences of initial and final state saturation phenomena, gluonic J \bar{J} loops, and jet quenching to particle

production in central (0-5%) Pb+Pb collisions at the LHC. Our study aims to investigate a set of observables sensitive to the dynamics of the collisions, covering both longitudinal and transverse degree of freedom. We present here the pseudorapidity multiplicity density per participant pair, and their centrality and energy dependence. Our study reveals a possible violation at $\sqrt{s_{\text{NN}}} = 2.76$ TeV of the *limiting fragmentation* observed in multiparticle production of charged particles up to top RHIC energy [39, 40]. Predictions for the nuclear modification factors (NMF) of charged particle (R_{AA}) and of identified particles ($R_{\text{AA}}^{\text{ID}}$) are also discussed. We emphasize the role of SCF effects and gluonic $\text{J}\bar{\text{J}}$ loops in understanding the *meson/baryon anomaly* at the LHC energy, which manifest in the (strange)baryon-meson ratios at intermediate and large transverse momenta and in NMF of identified particles ($R_{\text{AA}}^{\text{ID}}$).

II. OUTLINE OF HIJING/ $\bar{\text{B}}\bar{\text{B}}$ V2.0 MODEL.

A detailed description of the model can be found in Refs. [36–38]. The HIJING model is based on a two component geometrical model of mini-jet production and soft interaction and has incorporated nuclear effects such as *shadowing* (nuclear modification of the parton distribution functions) and *jet quenching*, via final state jet medium interaction. In the HIJING/ $\bar{\text{B}}\bar{\text{B}}$ v2.0 model [36, 37] we introduce new dynamical effects associated with long range coherent fields (*i.e.*, strong longitudinal color fields, SCF), including baryon junctions and loops [38, 41].

In order to achieve a quantitative description, within HIJING/ $\bar{\text{B}}\bar{\text{B}}$ v2.0 framework we have shown that combined effects of hard and soft sources of multiparticle production can reproduce the available data in the range $0.02 < \sqrt{s} < 7$ TeV only assuming a dependence of the effective string tension, κ , on c.m. energy (\sqrt{s}). We find [36] that the charged particle density in $p + p$ collisions can be well reproduced taking

$$\kappa(s) = \kappa_0 (s/s_0)^{0.06} \text{ GeV/fm} \approx Q_0 Q_{\text{sat}}(s), \quad (1)$$

where $\kappa_0 = 1$ GeV/fm is the vacuum string tension value, $s_0 = 1$ GeV² is a scale factor, and Q_0 is adjusted to give $\kappa(s) = 1.88$ GeV/fm at the RHIC energy $\sqrt{s} = 0.2$ TeV, and $Q_{\text{sat}}(s)$ is an internal momentum scale, also used in Color Glass Condensate (CGC) model [42, 43].

In a strong longitudinal color electric field, the heavier flavor suppression factor $\gamma_{Q\bar{Q}}$ varies with string tension via the well known Schwinger formula [44],

$$\gamma_{Q\bar{Q}} = \frac{\Gamma_{Q\bar{Q}}}{\Gamma_{q\bar{q}}} = \exp\left(-\frac{\pi(M_Q^2 - m_q^2)}{\kappa_0}\right) < 1 \quad (2)$$

for $Q = qq, s, c$ or b and $q = u, d$. Therefore, the above formula implies a suppression of heavier quark production according to $u : d : qq : s : c \approx 1 : 1 : 0.02 : 0.3 : 10^{-11}$ for the vacuum string tension $\kappa_0 = 1$ GeV/fm. For a color rope, on the other hand, the *average string tension* value increases due to *in-medium* effect. This increase is quantified in our calculations at RHIC and LHC energies, using a power law expression,

$$\kappa(s, A)_{RHIC} = \kappa(s)A^{0.087} \quad (3)$$

$$\kappa(s, A)_{LHC} = \kappa(s)A^{0.167} . \quad (4)$$

where the exponent has been fixed to provide a good description of the charged particle densities at mid-pseudorapidity (see below). With these increase string tensions the $Q\bar{Q}$ flavor pair production suppression factors, $\gamma_{Q\bar{Q}}$, approach unity in $A + A$ collisions. In our model this is the main mechanism for strange meson and hyperon enhancement.

It was shown recently [45] that charged-particle multiplicities measured in central heavy ion collisions at high energies may not directly determine the initial conditions as predicted by CGC models. In its simplest implementation it was generally assumed that there is a direct correspondence between the number of partons in the initial state and the number of particles in the final state [42, 43]. However, final state non-equilibrium production mechanisms generally increase the final multiplicity. In fact, in recent HIJING2.0 (that includes modern structure functions but without SCF and J \bar{J} loops) the enhancement of the multiplicity due to quenching of final minijets had to be turned off not to over predict the ALICE dN_{ch}/dy [9]. In HIJING/B \bar{B} 2.0 used here with super saturated Duke-Owens pdf's we find a consistent description of both p+p and Pb+Pb multiplicity when taking into account the extra multiplicity generated by minijet quenching.

As mentioned, in HIJING the string/rope fragmentation is the only *soft source* of multi-particle production and multiple minijets provide a semi-hard additional source that is computable within collinear factorized standard pQCD with initial and final radiation (DGLAP evolution [46]). Within the HIJING model, one assumes that nucleon-nucleon collisions at high energy can be divided into *soft* and *hard* processes with at least one pair of jet production with transverse momentum, $p_T > p_0(s)$. A cut-off (or saturation) scale $p_0(s)$ in the

final jet production has to be introduced below which the high density of initial interactions leads to a non-perturbative mechanisms which in the HIJING framework is characterized by a finite soft parton cross section σ_{soft} . The inclusive jet cross section σ_{jet} at leading order (LO) [47] is

$$\sigma_{\text{jet}} = \int_{p_0^2}^{s/4} dp_T^2 dy_1 dy_2 \frac{1}{2} \frac{d\sigma_{\text{jet}}}{dp_T^2 dy_1 dy_2}, \quad (5)$$

where,

$$\frac{d\sigma_{\text{jet}}}{dp_T^2 dy_1 dy_2} = K \sum_{a,b} x_1 f_a(x_1, p_T^2) x_2 f_b(x_2, p_T^2) \frac{d\sigma^{ab}(\hat{s}, \hat{t}, \hat{u})}{d\hat{t}} \quad (6)$$

depends on the parton-parton cross section σ^{ab} and parton distribution functions (PDF), $f_a(x, p_T^2)$. The summation runs over all parton species; y_1 and y_2 are the rapidities of the scattered partons; x_1 and x_2 are the light-cone momentum fractions carried by the initial partons. The multiplicative K factor ($K \approx 1.5 - 2$) account for the next-to-leading order (NLO) corrections to the leading order (LO) jet cross section [48, 49]. The parton distributions per nucleon in a nucleus (with atomic number A and charge number Z), $f_{a/A}(x, Q^2, r)$, are assumed to be factorizable into parton distributions in a nucleon ($f_{N/A}$) and the parton shadowing factor ($S_{a/A}$),

$$f_{a/A}(x, Q^2, r) = S_{a/A}(x, r) f_{N/A} \quad (7)$$

For the shadowing factor $S_{a/A}$ we take the parametrisation used in regular HIJING model [30, 50]. We also take into account the intrinsic transverse momentum and the transverse momentum broadening due to initial multiple scattering.

A saturation in the final state, i.e. of produced gluons, is possible, even without requirement of saturation in the initial state [51]. The largest uncertainty in mini-jet cross sections is the strong dependence on the minimum transverse momentum scale cut-off, $p_0(s)$. It was shown that an increased value (with c.m. energy \sqrt{s}) is required by the experimental data indicating that the *coherent interaction* becomes important. This might be taken also as an evidence of gluon final state saturation at very small x [9, 10]. With the Duke-Owens parameterization [52] of parton distribution functions, an energy independent cut-off scale $p_0 = 2 \text{ GeV}/c$ and a constant soft parton cross section $\sigma_{\text{soft}} = 57 \text{ mb}$ are found to reproduce the experimental data on the hadron central rapidity density in $p + p(\bar{p})$ collisions [36]. Here

we investigate for nucleus-nucleus collisions the effect of a new cut-off values $p_0(s)$, which has a power law energy dependence,

$$p_0(s) = 0.832 \sqrt{s_{\text{NN}}}^{0.191} \text{ GeV}/c \quad (8)$$

from $\sqrt{s_{\text{NN}}}=0.02$ TeV ($p_0 = 1.5$ GeV/ c) up to the highest energy $\sqrt{s_{\text{NN}}}=5.5$ TeV ($p_0 = 4.2$ GeV/ c). This energy dependence was shown to provide a good description for pseudorapidity distribution of charged particle at RHIC energies and allow also for a good extrapolations at LHC energies (see below, Sec. IIIA).

ALICE experiment at the LHC published first experimental data on the charged hadron multiplicity density at mid-rapidity in central (0-5%) Pb + Pb collisions at $\sqrt{s_{\text{NN}}}=2.76$ TeV [17]. In this experiment the collaboration also confirmed the presence of jet quenching [19] by studying R_{AA} . A measure of the jet quenching at large transverse momentum (p_T) is given by the ratio of particle yield in $A + A$ collisions to that in $p + p$ collisions, defined by

$$R_{AA} = \frac{(1/N_{\text{evt}}^{AA})d^2 N_{AA}/d^2 p_T dy}{N_{\text{coll}}(1/N_{\text{evt}}^{pp})d^2 N_{pp}/d^2 p_T dy} \quad (9)$$

where, N_{evt} is the number of events and N_{coll} is the number of binary nucleon-nucleon (NN) collisions. These results provide stringent constraints on the theoretical uncertainties in the bulk hadron production and have important consequences on theoretical predictions for jet quenching in Pb + Pb collisions at LHC energies.

For a parton a , the energy loss per unit distance can be expressed as $dE_a/dx = \epsilon_a/\lambda_a$, where ϵ_a is the radiative energy loss per scattering and λ_a the mean free path (mfp) of the inelastic scattering. For a *quark jet* at the top RHIC energy $(dE_q/dx)_{\text{RHIC}} \approx 1$ GeV/fm and mfp $(\lambda_q)_{\text{RHIC}} \approx 2$ fm [37]. The initial parton density is proportional to the final hadron multiplicity density. The charged particle density at mid-pseudorapidity at the LHC is a factor of 2.2 higher than that at the top RHIC energy [17]. Therefore, for a *quark jet* at the LHC the energy loss (mfp) should increase (decrease) by a factor of ≈ 2.0 and become $(dE_q/dx)_{\text{LHC}} \approx 2$ GeV/fm and mfp $(\lambda_q)_{\text{LHC}} \approx 1$ fm. Throughout this analysis we will consider the results with two sets of parameters for hard interactions:

$(dE/dx)_1$, i.e., $K = 1.5$; $dE_q/dx = 1$ GeV/fm; $\lambda_q = 2$ fm and

$(dE/dx)_2$, i.e., $K = 1.5$; $dE_q/dx = 2$ GeV/fm; $\lambda_q = 1$ fm.

Since there is always a coronal region with an average length of λ_q in the system where the produced parton jets will escape without scattering or energy loss, the suppression factor

can never be infinitely small. For the same reason, the suppression factor also depends on λ_q . It is difficult to extract information on both dE_q/dx and λ_q simultaneously from the measured spectra in a model independent way [53]. We show below that a constant radiative energy loss mechanism ($dE/dx=\text{const}$) as implemented in HIJING/B \bar{B} v2.0 model provides a good description of suppression at intermediate and larger p_T ($4 < p_T < 20$ GeV/ c) for charged particle in Pb+Pb collisions at the LHC.

III. RESULTS AND DISCUSSIONS

A. Multiplicity and Centrality Dependence

Charged-particle multiplicity density $(2dN_{\text{ch}}/d\eta)/N_{\text{part}}$ in central (0-5%) Pb+Pb collisions at $\sqrt{s_{\text{NN}}}=2.76$ TeV reported by the ALICE Collaboration is a factor of 2.2 higher than that observed in central Au+Au collisions at top RHIC energy. This value is larger than most of theoretical predictions, especially those from the CGC models [17]. Such large hadron multiplicity will have important consequences on the estimated *shadowing* and *jet quenching* in Pb+Pb collisions [56]. The value of $(2dN_{\text{ch}}/d\eta)/N_{\text{part}}$ at mid-pseudorapidity was reproduced by the HIJINGv2.0 model with a new set of PDFs [9] and has helped to constrain the gluon shadowing parameter in the model [10]. However, these calculations does not include the effects of *jet quenching*, which has been reported recently by ALICE [19], ATLAS [21] and CMS [22].

In previous studies of heavy ion collisions at RHIC [36, 37], the parameters of HIJING/B \bar{B} v2.0 model were adjusted in order to reproduce the measured charged particle multiplicity as well as (multi)strange particle production. In the present study of heavy ion collisions at the LHC we have to modify the values of these parameters in order to fit ALICE data [17]. As shown in Fig. 1 a good description (solid curve) of the measured charged particle multiplicity density at mid-pseudorapidity is obtained if the parameters $p_0(s) = 3.7$ GeV/ c , $\kappa(s, A) = 6.0$ GeV/fm, and $(dE/dx)_2$ (i.e., $K=1.5$; $dE_q/dx = 2$ GeV/fm; $\lambda_q = 1.0$ fm), are used.

The sensitivity of the calculations to the main parameters is illustrated by the dashed, dotted and solid curves. The dashed curve is obtained with the parameters used at RHIC energies: $p_0 = 2.0$ GeV/ c , $\kappa(s) = 2.6$ GeV/fm and $(dE/dx)_1$ (i.e., $K=1.5$; $dE_q/dx = 1$

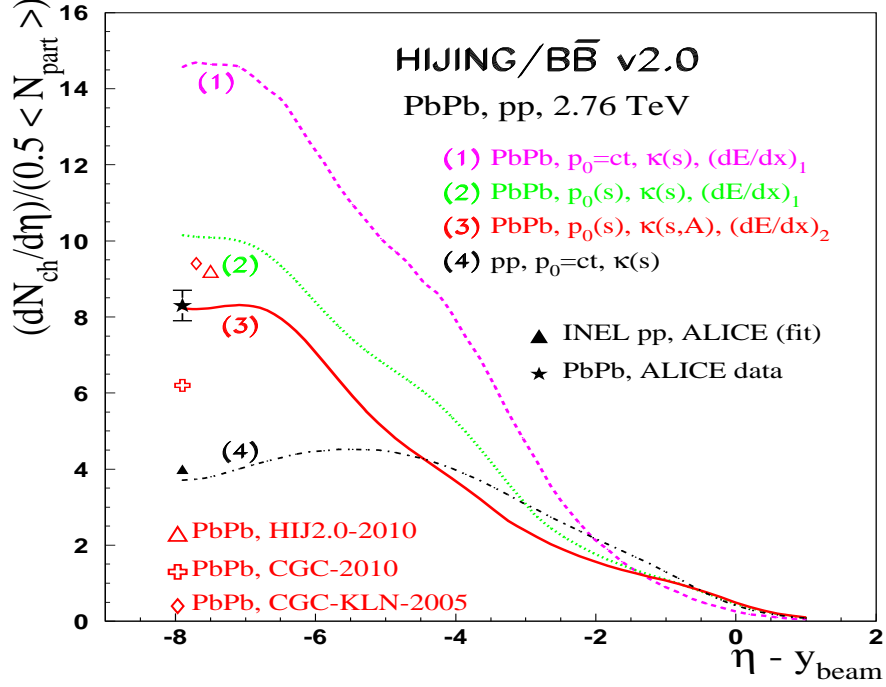


FIG. 1: (Color online) Comparison of HIJING/ $B\bar{B}$ v2.0 predictions for $(2dN_{\text{ch}}/d\eta)/N_{\text{part}}$ in central (0-5%) Pb+Pb collisions at $\sqrt{s_{\text{NN}}} = 2.76$ TeV. The results which give the best fit of the experimental value [17] are plotted as solid curve. The dotted and dashed curves illustrate the sensitivity to the main model parameters (see Sec. IIIA for explanation). The dot-dashed curve is obtained for $p + p$ NSD collisions at $\sqrt{s_{\text{NN}}} = 2.76$ TeV. The full triangle is the result obtained by interpolating data between at 2.36 and 7 TeV in Ref. [18]. Comparison with other model calculations are also shown. HIJING v2.0 model (open triangle from Ref. [10]), CGC models (open cross from Ref. [6]; open diamond from Ref. [4]).

GeV/fm; $\lambda_q = 2.0$ fm). The dotted curve is obtained if p_0 is increased to $p_0 = 3.7$ GeV/ c . Changing from set $(dE/dx)_1$ to $(dE/dx)_2$ results in a good description of data (solid curve). The dot dashed curve are the results for $p + p$ non-single diffractive (NSD) collisions at $\sqrt{s_{\text{NN}}}=2.76$ TeV and are obtained with the same set of parameters as described in Ref. [36].

The study of the dependence of observable $(2dN_{\text{ch}}/d\eta)/N_{\text{part}}$ on colliding system, center-of-mass energy and collision geometry is important to understand the relative contributions to particle production of hard scattering and soft processes. Multiparticle production of charged particles at RHIC energies exhibit the phenomenon of *limiting fragmentation* [39, 40]. This phenomenon is a consequence of Feynman scaling (if one views the collision in

the rest frame of one of the incident particles, the production process of the soft particles is independent of the energy or rapidity of the other particle.). The region in rapidity over which the particles appears to be independent of energy, increases with energy. It was argued that this phenomenon (called *extended longitudinal scaling*), is a direct manifestation of initial saturation which is assumed in CGC models [40].

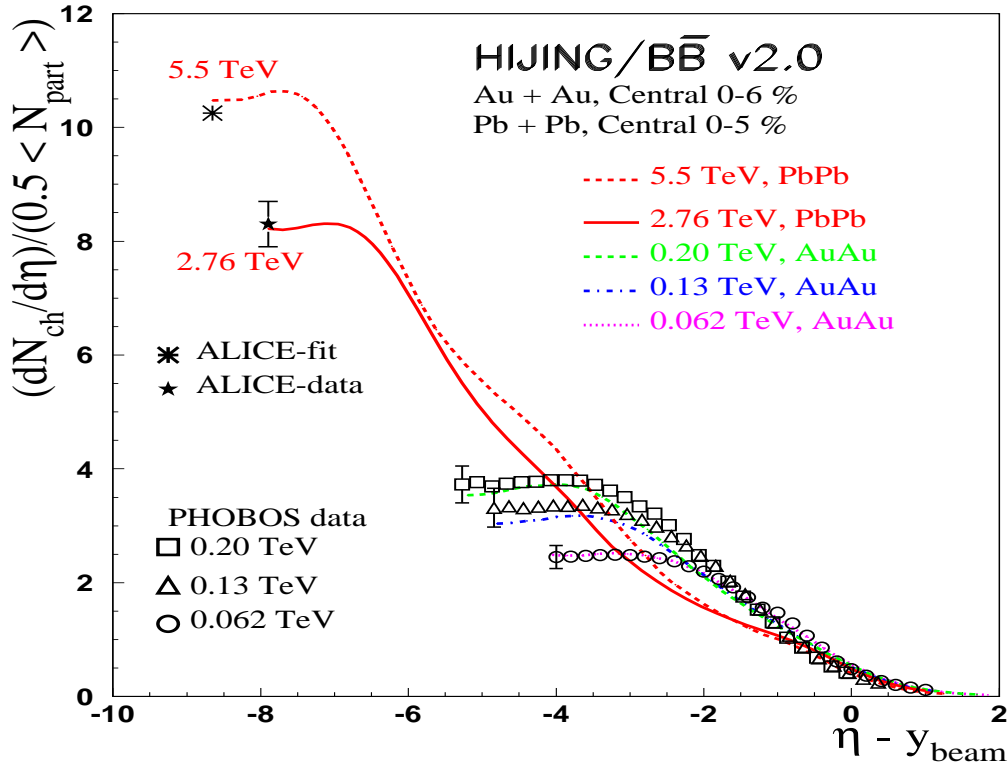


FIG. 2: (Color online) Comparison of HIJING/B \bar{B} v2.0 predictions for central charged particle density per participant pair produced in $A + A$ collisions at various energies. The data and theoretical results are plotted in the rest frame of one of the nuclei. The Au+Au data are from PHOBOS Collaboration [39, 40]. The statistical error bars are plotted only at mid-pseudorapidity for clarity. The Pb+Pb data at $\sqrt{s_{NN}}=2.76$ TeV (filled star) are from ALICE Collaboration [17]. The value at $\sqrt{s_{NN}}=5.5$ TeV (star) is obtained by a power law extrapolation from RHIC energies and 2.76 TeV data [17].

Figure 2 display the results for central (0-6%) Au+Au collisions at RHIC energies ($0.062 \text{ TeV} < \sqrt{s_{NN}} < 0.20 \text{ TeV}$) and in central (0-5%) Pb+Pb collisions at LHC energies ($\sqrt{s_{NN}}=2.76 \text{ TeV}$ and $\sqrt{s_{NN}}=5.5 \text{ TeV}$). Our calculations show that at RHIC energies the model predicts approximately a scaling seen also in data. However, some degree of vio-

lation of the phenomenon of *limiting fragmentation* and of the *extended longitudinal scaling* is predicted at both LHC energies. This violation is due to the partons hard scattering included in our model and missing in CGC models [3, 4, 6, 43].

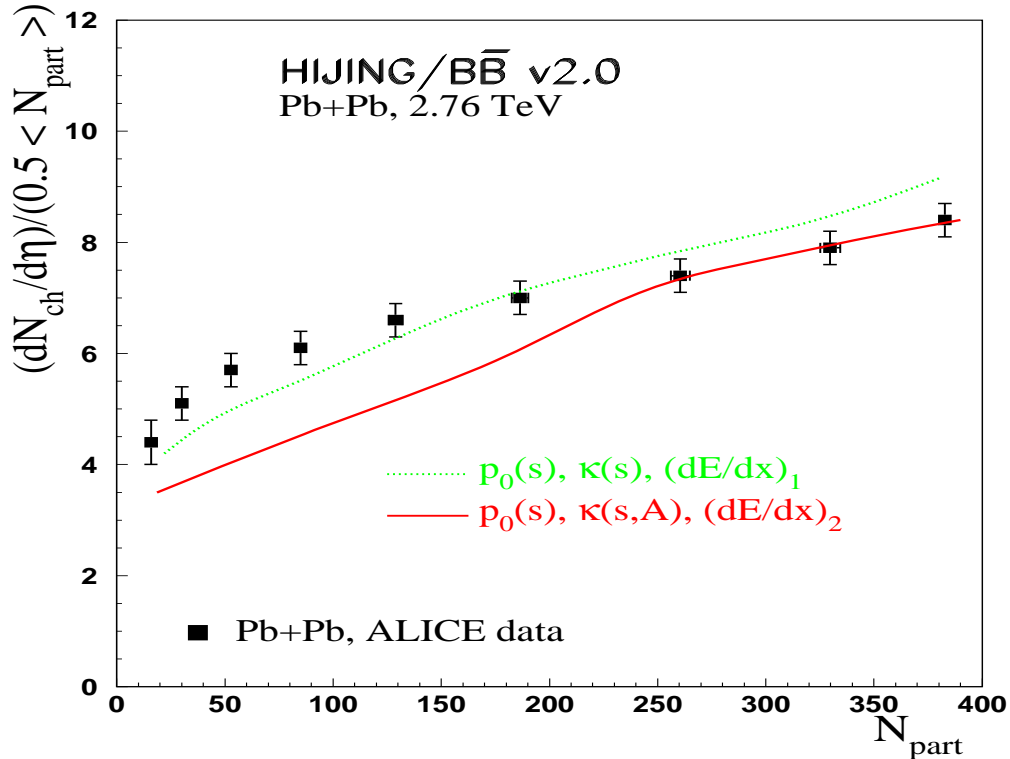


FIG. 3: (Color online) Comparison of HIJING/B \bar{B} v2.0 model calculations for charged particle multiplicity density at mid-pseudorapidity per participant pair $(2dN_{\text{ch}}/d\eta)/N_{\text{part}}$ as function of number of participants in Pb+Pb collisions at $\sqrt{s_{\text{NN}}} = 2.76$ TeV. The solid and dotted curves are the results obtained using the same set of parameters as in Fig. 1 (see text for explanations). All calculations include SCF effects and J \bar{J} loops. The data are from ALICE Collaboration [18] and the error bars include statistical and systematics uncertainties.

Figure 3 show the dependence of the pseudo-rapidity densities $((2dN_{\text{ch}}/d\eta)/N_{\text{part}})$ at mid-pseudo-rapidity, on the number of participant as measured by the ALICE Collaboration. The charged-particle density normalized per participant pair increases by a factor of roughly two from peripheral (70-80%) to central (0-5%) Pb+Pb collisions. The model calculations which have been tuned to high energy $p + p$ [36] and central (0-5%) Pb+Pb collisions data reasonably describe the central Pb+Pb data for $N_{\text{part}} > 250$. However, with the same set of parameters the model predicts a stronger rise with centrality than observed.

For peripheral collisions a better description is obtained if one use as parameters for the soft part $\kappa(s)$ (instead of $\kappa(s, A)$) successful in describing $p + p$ collisions and for hard scattering $p_0(s)$, $(dE/dx)_1$ as deduced from RHIC data. However, in this scenario the model overpredicts the absolute magnitude for central collisions ($N_{\text{part}} > 250$). These results indicate that the average energy loss per unit distance and the effective string tensions values should have an impact parameter (b) and a parton density dependence and a fine tuning is required to describe better these data. We leave this study to a future analysis.

B. Nuclear Modification factor for charged particle

In this paper, we make a simultaneous analysis of the high and low p_T part of charged-hadron p_T spectrum. Experiments at RHIC energies reported a suppression by a factor ≈ 5 compared with expectations from an independent superposition of nucleon-nucleon (NN) collisions [54, 55], interpreted as a strong evidence of formation of a strong coupling QGP (sQGP) in $A + A$ collisions. The jet quenching have also been confirmed in central (0-5%) $Pb + Pb$ collisions at the LHC [19, 21, 22].

Having a good description for charged particle multiplicity at mid-pseudorapidity, we analyze the model predictions on suppression of single hadron spectra in central (0-5%) $Pb+Pb$ collisions at the LHC. For other recent works discussing NMF of charged particle (R_{AA}) at the LHC, see recent references [56–62]. At the higher LHC energies a larger density of the medium is expected. This should lead to a larger suppression compared with that seen at RHIC energies. The observed nuclear modification factor R_{AA} [19] is characterized by the following behavior: a maximum at approximately $p_T = 2$ GeV/ c and a decrease with increasing p_T in the range 2-6 GeV/ c . For p_T greater that 6 GeV/ c , R_{AA} rises to reach a value of ≈ 0.4 at $p_T \approx 20$ GeV/ c .

The measured and predicted transverse momentum spectra at mid-pseudorapidity of primary charged particles in central (0-5%) $Pb+Pb$ collisions (upper solid histogram) and in $p + p$ collisions (lower solid histogram) at $\sqrt{s_{NN}}=2.76$ TeV are compared in Fig. 4(a). The HIJING/ $B\bar{B}$ v2.0 model describe fairly well the experimental p_T spectrum reported in Ref. [19]. The sensitivity of the calculations to the effective value of the string tension (κ) is shown by comparing the dotted ($\kappa(s) = 2.6$ GeV/fm) and the dashed ($\kappa(s, A) = 6.2$ GeV/fm) histograms. The sensitivity to the main hard scattering parameters is seen by

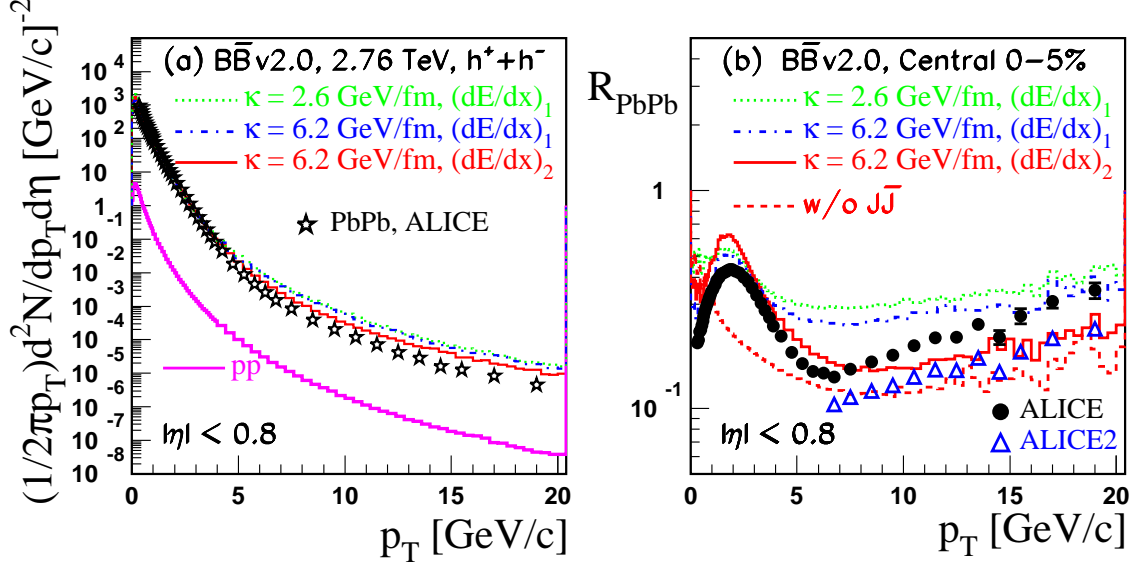


FIG. 4: (Color online) (a) Comparison of HIJING/ $B\bar{B}$ v2.0 predictions for the p_T distributions of primary charged particles at mid-pseudorapidity ($-0.8 < \eta < 0.8$) in central (0-5%) Pb+Pb collisions at $\sqrt{s_{NN}} = 2.76$ TeV. Theoretical calculations are for different values of parameters (see text for explanations). The p+p references values are shown as the lower solid histogram. (b) Theoretical calculations for nuclear modification factors R_{AA} are compared to data. The data (left and right panel) are from ALICE collaboration [19]. Error bars are statistical only. In part b) the open triangles are the results for R_{AA} at $p_T > 6.5$ GeV/c using alternative pp reference spectrum [19].

comparing the results obtained with the two sets $(dE/dx)_2$ (solid histograms) and $(dE/dx)_1$ (dash-dotted histograms). However, with the best set of parameters (solid histograms) the model still overestimate the high p_T tail of the p_T spectra. There are no experimental data on charged hadron spectra in $p + p$ collisions at $\sqrt{s_{NN}} = 2.76$ TeV. ALICE data on the suppression factor (R_{AA}) were obtained using a $p + p$ spectrum interpolated from their data at 0.9 TeV and 7 TeV. The open triangles in Fig. 4(b) represent the uncertainty in the interpolation method (see Ref. [19] for more details).

In medium modification of NMF (R_{AA}) is mainly caused by the energy loss suffered by partons while transversing the plasma due to collisions and radiation of gluons before they fragment and by the nuclear shadowing. To describe the nuclear shadowing we use in Eq. 5 the same functions as those used in regular HIJING model [30]. This has been shown to

be successful in explaining the results for R_{AA} at RHIC energies [37, 38]. The benchmark of any theoretical calculation is to describe the shape seen at low $p_T < 6$ GeV/ c in R_{AA} . We can explain the shape and the presence of a maximum at approximately $p_T = 2$ GeV/ c as a specific interplay between non-perturbative (SCF effects) and perturbative (gluonic $J\bar{J}$ dynamical loops) mechanisms contribution. The results without $J\bar{J}$ loops (dashed histogram) shown in Fig. 4(b) strongly underestimate the experimental values of R_{AA} in this p_T range.

Since we are mostly interested in the overall effects, we concentrate also on the modification of high p_T hadron spectra due to an assumed total energy loss related to the averaged energy loss per unit distance. The mechanism which gives a constant energy loss per collisions is seen to describe quite well the data (within the systematics uncertainties) over the largest p_T window of 6 - 20 GeV/ c . R_{AA} increases with p_T because of the constant energy loss assumed here. For a constant energy loss per collisions (ΔE_T) the ratio $\Delta E_T/E_T$ becomes smaller for larger E_T , thus the suppression is expected to decrease with increasing p_T . Here, the energy loss per collisions is about twice as large and the mean free path of parton-parton interactions is smaller by a factor of roughly two as compared with that used at the top RHIC energy. These analysis can provide information about the average total energy loss the parton suffers during its interaction with the medium. However, a more quantitative analysis should be performed with the knowledge of the dynamical evolution of the system which is beyond the scope of this paper.

C. Baryon/Meson anomaly at the LHC

Identified particles at high p_T provide direct sensitivity to differences between quark and gluon fragmentation [63]. Proton and pion production at high p_T is expected to have significant contributions from quark fragmentation while anti-protons result mainly from gluon fragmentation [53]. Therefore, the ratios \bar{p}/π^- , p/π^+ are sensitive to the possible color charge dependence of energy loss. Systematic measurements of identified particle spectra in $p + p$ and Au+Au collisions at RHIC energies [63–67] in the p_T region 2-12 GeV/ c show a significant suppression with respect to binary scaling. However, protons and anti-protons are less suppressed than pions at intermediate p_T (2-9 GeV/ c). For $p_T > 2$ GeV/ c , the ratios \bar{p}/π^- and p/π^+ does not depend strongly on energy and they are higher in central than in peripheral collisions. In addition to be sensitive to quark and gluon jet production

these are also sensitive to baryon transport properties and the energy density.

Moreover, the meson/baryon ratio suggest that baryon and anti-baryon production may dominate the moderate high p_T flavor yields. These findings challenge various models incorporating jet quenching [53],[68], and/or constituent quark coalescence [69, 70]. The fact that in the intermediate p_T region the p/π^+ and \bar{p}/π^- ratios are close to unity (baryon/meson anomaly) has been attributed to either quark coalescence or to novel baryon transport dynamics [68], based on topological gluon field configurations [71–74]. However, the baryon junction model predictions from Ref. [68] are not in agreement with data [65].

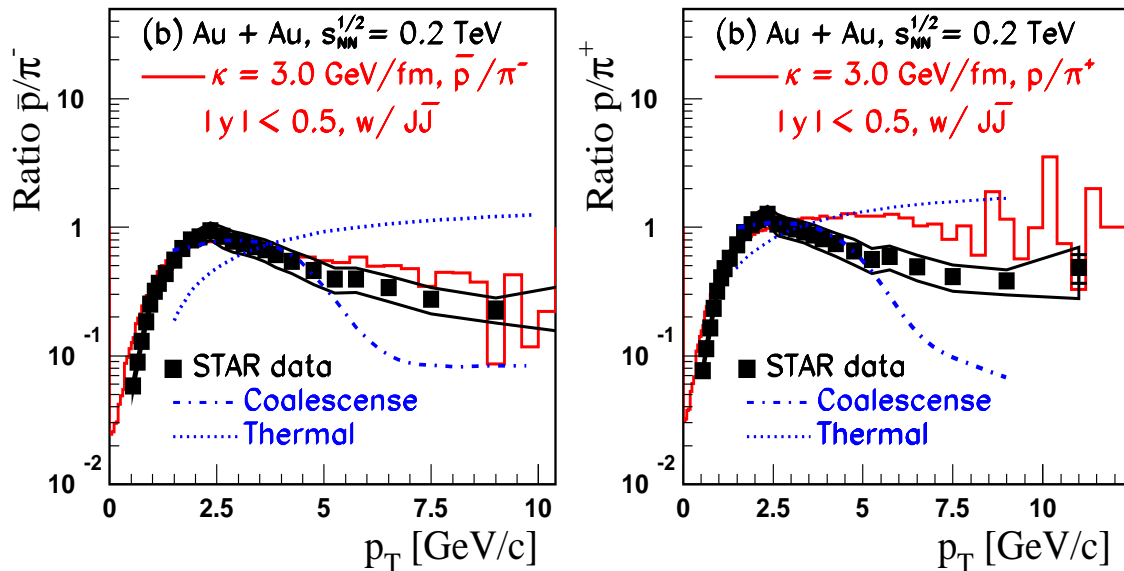


FIG. 5: (Color online) Comparison of HIJING/ $B\bar{B}$ v2.0 predictions (solid histogram) for ratios \bar{p}/π^- (left panel) and p/π^+ (right panel) to STAR data [65] and to coalescence (dot dashed curves) and thermal (dotted curves) model calculations from Ref. [69]. The error bars include only statistical uncertainties and systematics are introduced by thin continue curves.

Figure 5 displays the mid-rapidity ratios for central (0-12%) Au+Au collisions [65] at $\sqrt{s_{NN}} = 0.2$ TeV in comparison with model predictions. The observed ratios peak at $p_T \approx 2-3$ GeV/ c with value close to unity and then decrease with increasing p_T and approach the ratios observed in $p+p$ collisions at $p_T > 6$ GeV/ c . The results presented (solid histograms) include SCF and $J\bar{J}$ loops contributions. The calculations based on quark coalescence (dot-dashed curves) and thermal models (dotted curves) from Ref. [69] are also plotted. The grouping of particle production according to the number of constituent quarks has been

attributed to quark coalescence from a collective partonic medium [70]. The coalescence models [69, 70] can qualitatively describe these data at intermediate $p_T < 5$ GeV/ c , but strongly under-predict the results at high p_T , due to fragmentation functions used within the model. To the contrary, the thermal model calculations [69] strongly overestimate the data at high p_T . Our model provides an alternative explanation to the baryon/meson anomaly. The reason is a specific interplay of contributions from SCF effects and dynamical $J\bar{J}$ loops. The predictions of our model are in good agreement with data up to the highest p_T , in the limit of systematics uncertainties. However, the model overestimate the p/π^+ ratio for $3 < p_T < 6$ GeV/ c , while it provides a good description for protons (p), it under-predicts the pions (π^+) spectrum in this region. Since the ratio \bar{p}/π^- is well described by the model, these calculations could indicate that the fragmentation functions for π^+ productions are not well estimated.

With the best set of parameters used to describe charged particle production in central (0-5%) and peripheral (70-80%) Pb+Pb collisions at $\sqrt{s_{NN}} = 2.76$ TeV (see Sec. IIIA), we present in Fig. 6 the model predictions for centrality dependence of the non-strange baryon/meson ratio (left panel) and of strange baryon/meson ratio (right panel). Our model predicts that these ratios does not depend strongly on energy and centrality. The model also predicts that the baryon/meson anomaly will persist up to high p_T . For central (0-5%) Pb+Pb collisions at $\sqrt{s_{NN}} = 2.76$ TeV, in a scenario with jet quenching and shadowing as explained in Sec. II, but without $J\bar{J}$ loops and SCF effects the \bar{p}/π^- ratio in the region of the maximum ($2 < p_T < 3$ GeV/ c) is 0.07. We have studied the sensitivity of the results to the $J\bar{J}$ loops and SCF effects. Considering only $J\bar{J}$ loops leads to an increase by a factor of two, and taken into consideration only SCF effects lead to an increase up to a factor of ≈ 14 for the \bar{p}/π^- ratio. Note, that an important fraction of this increase is also due to much stronger quench of pions in comparison with that of anti-protons, as we will show below (see Fig. 8).

The ALICE and CMS detectors are designed to perform measurements in the high-multiplicity environment of central Pb+Pb collisions at the LHC [34], [35]. To isolate QGP signatures in heavy-ion collisions, understanding the particle production properties from NN interactions is necessary. In addition, the transverse momentum spectrum in $p + p$ collisions serve as a baseline to study possible suppression (i.e., nuclear modification factor $R_{AA}^{ID}(p_T)$) in heavy ion collisions. This stresses the need for reference $p + p$ measurements

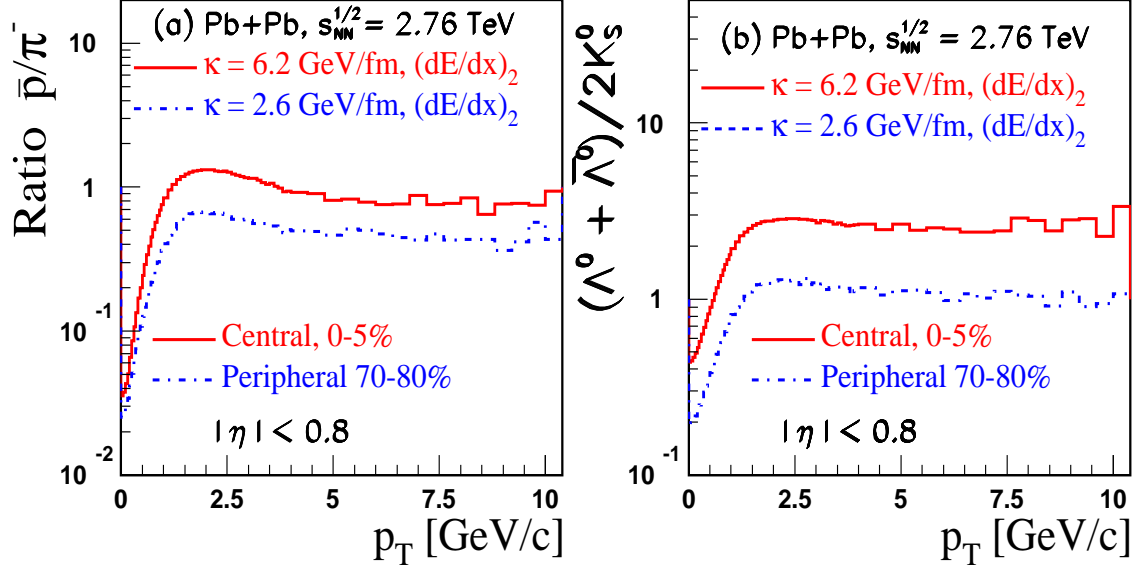


FIG. 6: (Color online) Predictions for centrality dependence of (non)strange baryon/meson ratios from HIJING/B \bar{B} v2.0. The results include SCF effects and J \bar{J} loops. In each figure the histograms correspond to two value of centrality and the associated string tension.

at LHC energies of identified particles. In a previous paper [36] we show that the large (strange)baryon-to-meson ratios measured at Tevatron (1.8 and 1.96 TeV) and LHC energies (0.9 and 7 TeV) are well described in the framework of HIJING/B \bar{B} v2.0 model. Recently, the CDF reported a set of measurements of inclusive invariant p_T differential cross sections of hyperons with different strangeness, Λ^0 (quark content (uds)), Ξ^- (dss), and Ω (sss). These data are obtained for central region with pseudorapidity range $-1 < \eta < 1$ and p_T up to 10 GeV/ c , and are used to test our model calculations which include SCF effects and J \bar{J} loops.

In a scenario with SCF effects (i.e., considering $\kappa = \kappa(s)$ [36]) the increase of the yield is higher for multi-strange hyperons (Ξ^-, Ω^-) than for strange hyperon (Λ^0), in comparison with the results obtained without SCF effects (i.e., taking vacuum string tension value $\kappa_0 = 1$ GeV/fm). The increase of the yield with strangeness content is due to an increase of strange quark suppression (γ_s), obtained from a power law dependence of effective string tension values, $\kappa(s) = \kappa_0 (s/s_0)^{0.06}$ GeV/fm (see Fig. 2 from Ref. [36]). Figure 7 shows the predicted p_T differential cross sections (left panel) for the three hyperon resonances in comparison with data. The plots on the right side of Fig. 7 show the ratio of the p_T differential cross sections

for Ξ^-/Λ^0 and Ω^-/Λ^0 . In the limit of the experimental error (systematics+statistical) our model describes well these data.

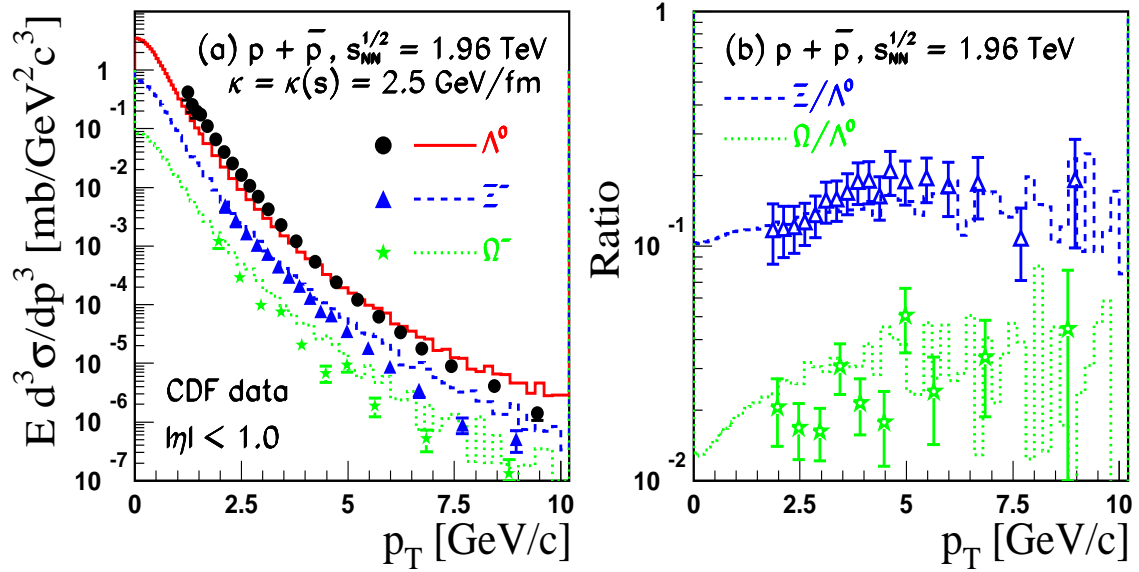


FIG. 7: (Color online) Part (a) Comparison of HIJING/B \bar{B} v2.0 predictions for the P_T differential cross sections of Λ^0 (solid), Ξ (dashed), and Ω (dotted histograms). The calculations are for $p + \bar{p}$ collisions at 1.96 TeV and include SCF effects and $J\bar{J}$ loops as in ref. [36]. Part (b) The ratios Ξ/Λ^0 (dashed histogram) and Ω/Λ^0 (dotted histogram). The data are from CDF Collaboration [33]. Only statistical uncertainties are shown.

Strangeness enhancement, strong baryon transport, and increase of intrinsic transverse momentum are all expected consequences of longitudinal SCF effects. These are modeled in our microscopic models as an increase of the effective string tension that controls quark-anti-quark ($q\bar{q}$) and diquark-anti-diquark ($qq\bar{q}\bar{q}$) pair creation rates and the strangeness suppression factors (γ_s). The predictions in central Pb+Pb collisions for initial energy density and temperature are $\epsilon_{\text{LHC}} \approx 200$ GeV/fm 3 , and $T_{\text{LHC}} \approx 500$ MeV, respectively [75]. Both values would lead in the framework of our model to an estimated increase of the average value of string tension to $\kappa_{\text{LHC}} \approx 5 - 6$ GeV/fm [2], consistent with our parameterization from Eq. 4.

The predictions for NMF of identified particles ($R_{AA}^{\text{ID}}(p_T)$) are presented in Fig. 8 for non-strange particles (left panel) and (multi)strange particles (right panel). From the results of our model we conclude that baryon/meson anomaly, i.e., different meson and baryon

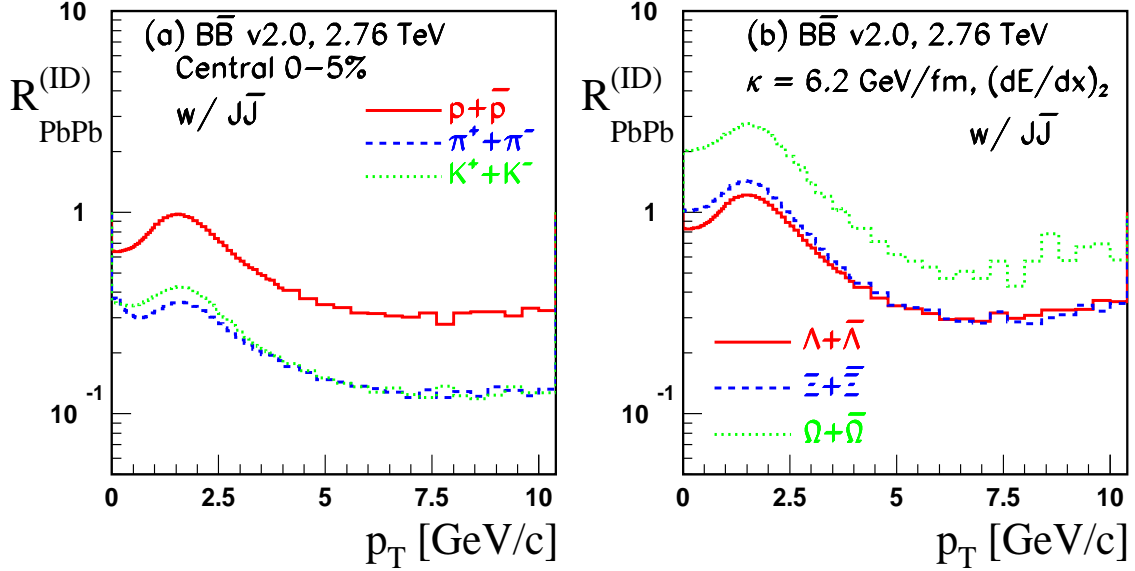


FIG. 8: (Color online) Predictions from HIJING/ $\bar{B}\bar{B}$ v2.0 model for nuclear modification factors R_{AA}^{ID} of identified particles at mid-pseudorapidity ($-0.8 < \eta < 0.8$) in central (0-5%) Pb+Pb collisions at $\sqrt{s_{NN}} = 2.76$ TeV. The results include SCF effects and $J\bar{J}$ loops. Left: pions, kaons and protons. Right: hyperons Λ, Ξ, Ω .

suppression, will persist in central Pb+Pb collisions at the LHC energy $\sqrt{s_{NN}} = 2.76$ TeV up to a higher value of transverse momentum. The $R_{AA}^{ID}(p_T)$ also exhibit an ordering with strangeness content at low and intermediate p_T , the increase of the yield being higher for multi-strange hyperons than that for (non)strange baryons (i.e., $R_{PbPb}(\Omega) > R_{PbPb}(\Xi) > R_{PbPb}(\Lambda) > R_{PbPb}(p)$). This prediction could be verified by the future planned experiments at the LHC.

IV. SUMMARY AND CONCLUSIONS

We have studied the influence of strong longitudinal color fields and of possible multi-gluon $J\bar{J}$ loops dynamics in particle production in Pb+Pb collisions at 2.76 TeV. We have investigated a set of observables sensitive to the dynamics of the collisions, covering both longitudinal and transverse degree of freedom. A detailed comparison with available experimental data from the LHC has been performed.

We find that the inclusion of the multiple minijet source limits the growth of the string

tension $\kappa(s)$ to be approximately linear as a function of saturation scale Q_{sat} , in contrast to recent approaches [43] where $\kappa(s)$ scales as Q_{sat}^2 . The reason is that in the CGC model the collinear factorized minijet mechanism is suppressed by geometric scaling to much higher p_T . Moreover, an increase with A , due to an increase in initial energy density is necessary in order to better describe new ALICE data.

We have shown that Strong color field (SCF) could play an important role in particle production at mid-rapidity in heavy-ion collisions. The mechanisms of hadron production are very sensitive to the early phase of the collisions, when fluctuations of the color field strength are highest. Strong Color Field effects are modeled by varying the effective string tension that controls the quark-anti-quark ($q\bar{q}$) and diquark-anti-diquark ($qq\bar{q}\bar{q}$) pair creation rates and strangeness suppression factors (γ_s). SCF also modify the fragmentation processes resulting in an increase of (strange)baryons.

We show that baryon/meson anomaly manifest in an increase of baryon-to-meson ratios as well as in different suppression of meson and baryon and persist up to high p_T ($p_T < 10$ GeV/ c). We show also that the $R_{AA}^{\text{ID}}(p_T)$ exhibit an ordering with strangeness content at low and intermediate p_T , the increase of the yield being higher for multi-strange hyperons than that for (non)strange baryons.

V. ACKNOWLEDGMENTS

Acknowledgments: We thank S. Das Gupta, S. Jeon, and P. Levai for fruitful discussions and support. VTP acknowledges the use of computer facilities at Columbia University, New York, where part of these calculations were performed. This work was supported by the Natural Sciences and Engineering Research Council of Canada. This work was also supported by the Division of Nuclear Science, of the U. S. Department of Energy under Contract No. DE-AC03-76SF00098 and DE-FG02-93ER-40764.

-
- [1] N. Armesto *et al.*, J. Phys. G **35**, 054001 (2008).
[2] N. Armesto *et al.*, J. Phys. G **35**, 054001 (2008); V. Topor Pop *et al.*, *ibid.* **35**, 15 (2008); V. Topor Pop *et al.*, *ibid.* **35**, 57 (2008).

- [3] J. L. Albacete, J. Phys. Conf. Ser. **270** (2011), Proceedings of the International Conference Hot Quarks 2010, 21-26 Jun 2010, La Londe les Maures, French Riviera, France, Edited by M. Bleicher *et al.*.
- [4] D. Kharzeev, E. Levin, M. Nardi, Nucl. Phys. **A747**, 609 (2005).
- [5] N. Armesto, C. A. Salgado, U. A. Wiedemann, Phys. Rev. Lett. **94**, 022002 (2005).
- [6] E. Levin, A. H. Rezaeian, Phys. Rev. D **82**, 054003 (2010).
- [7] E. Levin, A. H. Rezaeian, Phys. Rev. D **82**, 014022 (2010).
- [8] E. Levin, A. H. Rezaeian, Phys. Rev. D **83**, 114001 (2011).
- [9] W. -T. Deng, X. -N. Wang, R. Xu, Phys. Rev. C **83**, 014915 (2011).
- [10] W. T. Deng, X. -N. Wang and R. Xu, arXiv:1011.5907 [nucl-th].
- [11] P. Bozek, M. Chojnacki, W. Florkowski, B. Tomasik, Phys. Lett. **B694**, 238 (2010).
- [12] E. K. G. Sarkisyan, A. S. Sakharov, Eur. Phys. J. C **70**, 533 (2010).
- [13] T. J. Humanic, [arXiv:1011.0378 [nucl-th]].
- [14] J. Xu, C. M. Ko, Phys. Rev. C **83**, 034904 (2011).
- [15] M. Mitrovski, T. Schuster, G. Graf, H. Petersen, M. Bleicher, Phys. Rev. C **79**, 044901 (2009).
- [16] F. W. Bopp, R. Engel, J. Ranft, S. Roesler, [arXiv:0706.3875 [hep-ph]].
- [17] K. Aamodt *et al.* [ALICE Collaboration], Phys. Rev. Lett. **105**, 252301 (2010).
- [18] K. Aamodt *et al.* [ALICE Collaboration], Phys. Rev. Lett. **106**, 032301 (2011).
- [19] K. Aamodt *et al.* [ALICE Collaboration], Phys. Lett. **B696**, 30 (2011).
- [20] K. Aamodt *et al.* [ALICE Collaboration], [arXiv:1011.3914 [nucl-ex]].
- [21] G. Aad *et al.* [ATLAS Collaboration], Phys. Rev. Lett. **105**, 252303 (2010).
- [22] S. Khachatryan *et al.* [CMS Collaboration], [arXiv:1102.1957 [nucl-ex]].
- [23] J. Casalderrey-Solana, J. G. Milhano, U. A. Wiedemann, J. Phys. G **38**, 035006 (2011).
- [24] M. H. Seymour, to appear in the Proceedings of Physics at LHC 2010 (PHLC2010), 7-12 June 2010, Hamburg Germany, arXiv:1008.2927 [hep-ph].
- [25] R. Sassot, P. Zurita, M. Stratmann, Phys. Rev. D **82**, 074011 (2010).
- [26] K. Werner, I. Karpenko, T. Pierog, Phys. Rev. Lett. **106**, 122004 (2011).
- [27] B. Andersson, G. Gustafson, B. Nilsson-Almqvist, Nucl. Phys. **B281**, 289 (1987); B. Nilsson-Almqvist, E. Stenlund, Comput. Phys. Commun. **43**, 387 (1987).
- [28] A. Capella, U. Sukhatme, J. Tran Thanh Van, Z. Phys. **C3**, 329-337 (1979); J. Ranft, Phys. Rev. D **37**, 1842 (1988).

- [29] H. -U. Bengtsson, T. Sjostrand, *Comput. Phys. Commun.* **46**, 43 (1987).
- [30] X. -N. Wang and M. Gyulassy, *Comput. Phys.* **83** (1994) 307; X. -N. Wang, *Phys. Rep.* **280**, 287 (1997).
- [31] P. Koch, B. Muller and J. Rafelski, *Phys. Rep.* **142**, 321 (1986).
- [32] A. Andrichetto *et al.* [WA85 and WA94 Collaboration], *J. Phys. G* **25**, 209-216 (1999).
- [33] T. Aaltonen *et al.* [CDF Collaboration], [arXiv:1101.2996 [hep-ex]].
- [34] K. Aamodt *et al.* [ALICE Collaboration], *Eur. Phys. J. C* **71**, 1655 (2011).
- [35] V. Khachatryan *et al.* [CMS Collaboration], *JHEP* **1105**, 064 (2011).
- [36] V. Topor Pop, M. Gyulassy, J. Barrette, C. Gale and A. Warburton, *Phys. Rev. C* **83**, 024902 (2011).
- [37] V. Topor Pop, M. Gyulassy, J. Barrette, C. Gale, S. Jeon and R. Bellwied, *Phys. Rev. C* **75**, 014904 (2007) (and references therein).
- [38] V. Topor Pop, M. Gyulassy, J. Barrette, C. Gale, *Phys. Rev. C* **72**, 054901 (2005).
- [39] W. Busza *et al.* [PHOBOS Collaboration], *Nucl. Phys.* **A830**, 35c (2009).
- [40] W. Busza, *Nucl. Phys.* **A854**, 57-63 (2011).
- [41] G. Ripka (ed.), *Lecture Notes in Physics* (Springer, Berlin, 2004), Vol. **639**, 138 (2004).
- [42] F. Gelis, T. Lappi and L. McLerran, *Nucl. Phys.* **A828**, 149 (2009); T. Lappi and L. McLerran, *Nucl. Phys.* **A772**, 200 (2006).
- [43] L. McLerran and M. Praszalowicz, *Acta Phys. Polon. B* **41**, 1917 (2010).
- [44] J. S. Schwinger, *Phys. Rev.* **82**, 664 (1951).
- [45] R. Baier, A. H. Mueller, D. Schiff, D. T. Son, [arXiv:1103.1259 [nucl-th]].
- [46] G. Altarelli and G. Parisi, *Nucl. Phys.* **B126**, 298 (1977).
- [47] E. Eichten, I. Hinchliffe, K. D. Lane and C. Quigg, *Rev. Mod. Phys.* **56**, 579 (1984) [Addendum-*ibid.* **58**, 1065 (1986)].
- [48] K. J. Eskola, X. -N. Wang, *Int. J. Mod. Phys.* **A10**, 3071 (1995).
- [49] J. M. Campbell, J. W. Huston, W. J. Stirling, *Rept. Prog. Phys.* **70**, 89 (2007).
- [50] X. -N. Wang, M. Gyulassy, *Phys. Rev. Lett.* **68**, 1480 (1992).
- [51] K. J. Eskola, *Nucl. Phys.* **A698**, 78c (2002).
- [52] D. W. Duke and J. F. Owens, *Phys. Rev. D* **30**, 49 (1984).
- [53] X. -N. Wang, *Phys. Rev. C* **58**, 2321 (1998).
- [54] J. Adams *et al.* [STAR Collaboration], *Nucl. Phys.* **A757**, 102 (2005).

- [55] K. Adcox *et al.* [PHENIX Collaboration], Nucl. Phys. **A757**, 184 (2005).
- [56] X. -F. Che, T. Hirano, E. Wang, X. -N. Wang, H. Zhang, [arXiv:1102.5614 [nucl-th]].
- [57] A. Majumder, C. Shen, [arXiv:1103.0809 [hep-ph]].
- [58] T. Renk, H. Holopainen, R. Paatelainen, K. J. Eskola, [arXiv:1103.5308 [hep-ph]].
- [59] A. Kormilitzin, E. Levin, A. H. Rezaeian, Nucl. Phys. **A860**, 84-101 (2011).
- [60] D. K. Srivastava, J. Phys. G **38**, 055003 (2011).
- [61] W. A. Horowitz, M. Gyulassy, [arXiv:1104.4958 [hep-ph]].
- [62] P. Levai, [arXiv:1104.4162 [hep-ph]].
- [63] B. I. Abelev *et al.* [STAR Collaboration], Phys. Rev. Lett. **97**, 152301 (2006).
- [64] B. I. Abelev *et al.* [STAR Collaboration], Phys. Rev. C **79**, 034909 (2009).
- [65] B. I. Abelev *et al.* [STAR Collaboration], Phys. Lett. **B655**, 104 (2007).
- [66] S. S. Adler *et al.* [PHENIX Collaboration], Phys. Rev. Lett. **91**, 172301 (2003).
- [67] J. Adams *et al.* [STAR Collaboration], Phys. Rev. Lett. **92**, 052302 (2004).
- [68] I. Vitev, M. Gyulassy, Phys. Rev. C **65**, 041902 (2002).
- [69] R. J. Fries, B. Muller, C. Nonaka, S. A. Bass, Phys. Rev. C **68**, 044902 (2003).
- [70] R. J. Fries, V. Greco, P. Sorensen, Ann. Rev. Nucl. Part. Sci. **58**, 177 (2008) (and references therein).
- [71] G. C. Rossi, G. Veneziano, Nucl. Phys. **B123**, 507 (1977).
- [72] L. Montanet, G. C. Rossi, G. Veneziano, Phys. Rept. **63**, 149 (1980).
- [73] D. Kharzeev, Phys. Lett. **B378**, 238 (1996).
- [74] S. E. Vance, M. Gyulassy, Phys. Rev. Lett. **83**, 1735 (1999).
- [75] B. Muller, Nucl. Phys. **A783**, 403 (2007).